Flomeko 2000 - IMEKO TC9 Conference
Salvador, Bahia, BRAZIL
4-8 June, 2000

NUMERICAL STUDY OF CRITICAL FLOW IN SMALL ORIFICES

Paulo J. S. Jabardo and Kazuto Kawakita

IPT-Institute for Technological Research
Cidade Universitária, São Paulo-SP, BRAZIL

Abstract: *This paper presents a numerical investigation of critical flow in small cylindrical orifices. Microorifices with diameters ranging from 16 to 423μm with length to diameter ratios (L/D) ranging from 0,6 to 16 were simulated using a numerical solver. Flow simulations were carried out under several back to upstream pressure ratios (P_b/P_0) under pressurized (increasing upstream pressure P_0) and vacuum (decreasing back pressure P_b) modes of operation. Numerical results were validated by comparing calculated flow rates with experimental data. This comparison showed a good agreement between simulation and experimental data. Results also showed that, when operating with small diameter orifices under vacuum conditions, both the Reynolds number and the volumetric flow rate remain constant at critical flow regime. However, when operating under pressure, the volumetric flow rate refered to the upstream stagnation conditions does not stabilise even at critical flow conditions, and the Reynolds number increases by decreasing the back to upstream pressure ratio.*

Keywords: orifice, microorifice, capillary, critical flow, compressible flow

1 INTRODUCTION

Critical flow through orifices and nozzles has been a subject of extensive experimental and theoretical research over the years. These studies, however, are usually limited to relatively large sized critical elements, in most cases orifices or nozzles presenting bore or throat diameters larger than 1mm, and capable of supplying fairly large gas flow rates. In this scenery, application of choked flow in microstructures such as capillaries, nozzles and orifices would certainly help measuring and controlling very low gas flow rates, even of the order of cm^3/min.

Although some experimental data obtained using small-scale orifices operating at critical flow regime is reported in the literature (Kawakita [1]), very little information is available concerning the microstructure of the flow itself. Due to the small dimensions involved, velocity field measurements or practical flow visualization techniques are extremely difficult to be applied to these devices. As a result, a thorough understanding of the flow pattern involved in such a flow is almost impossible by experimental means. An alternative solution to this problem is the numerical simulation of the flow. This approach allows the determination of the velocity, temperature and pressure fields inside the microorifice, thus allowing a better understanding of the flow pattern. Hence, in this investigation flow through several microorifices with different lengths and diameters were simulated at different pressure ratios in two basic modes of operation:

- Operation under pressure: increasing upstream pressure (P_0) while maintaining back pressure (P_b) constant.
- Operation under vacuum: decreasing back pressure (P_b) while maintaining upstream pressure (P_0) constant.

Simulations were carried out using the numerical solver FLUENT. This computer software allows the solution of the Navier-Stokes equations for fluid flows. Using this solver, compressible viscous flows (laminar and turbulent, using *k-e* models) with heat transfer may be simulated in complex geometries. In large sized orifices and nozzles, simple one-dimensional analysis can be carried out with good results. In some cases, even isoentropic relations can give accurate results, for instance, flows inside nozzles. As the dimensions of the flow structure decreases, so does the Reynolds number. As a result, the relative boundary layer thickness increases and thus, a one-dimensional model of the flow becomes too inaccurate to represent the flow pattern.

2 MATHEMATICAL MODEL OF THE FLOW

The Navier-Stokes equations can be used to model the flow in orifices and capillaries even when small dimensions are involved. The lower limit of applicability of this model is given by the Knudsen number (*Kn*). The following relation from Shapiro [2] represents the Knudsen number:

$$Kn = 1{,}26\sqrt{\gamma}\,\frac{M}{Re} \tag{1}$$

In this equation, *M* is the Mach number, *Re* is the Reynolds number and γ is the ratio of specific heats C_p/C_v of the gas. For large values of Knudsen number ($Kn > 0{,}01$), the continuum hypothesis used by the Navier-Stokes equations is no longer valid. Throughout this investigation Knudsen numbers were maintained at small values and, therefore, the Navier-Stokes equations are applicable. In fact, the worst case refers to a Kn=0,03, which is slightly higher than the upper limit of validity of the continuum hypothesis.

Up to date, there is no general solution for the Navier-Stokes equations and therefore, numerical solution is necessary. Even when using numerical methods, due to the extremely complex nature of the flow equations, some simplifications are necessary to reduce computational costs. Since this paper deals only with cylindrical microorifices, it is reasonable to use an axisymetric coordinate system, and doing so, every flow variable becomes a function of the distance from the axis for each specific position along this axis.

2.1 Domain discretization

FLUENT uses a finite volume formulation to solve the Navier-Stokes equations. The finite volume solves the flow equations by applying the integral equations of fluid dynamics (conservation of mass, momentum and energy) to different volumes (elements) of the domain. The finite volume method requires an appropriate discretization of the domain (mesh) and figure 1 shows a typical mesh used in this work.

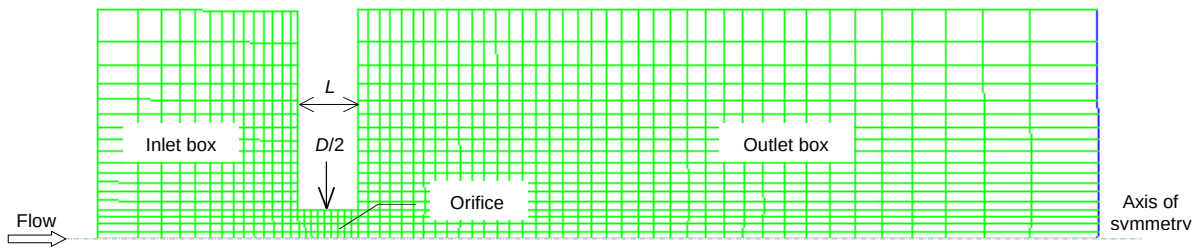

Figure 1. Typical mesh used for the simulation. In this case the mesh represents an orifice with length to diameter ratio (*L*/*D*) of 0,6.

Notice in figure 1 the "boxes" at the inlet and outlet of the orifice. These boxes are essential since they allow the proper development of streamlines and settling of pressure upstream and downstream of the orifice. The inlet box physically represents the section where upstream pressure and temperature at stagnation conditions are measured. The outlet box represents the section where back pressure and temperature are measured.

2.2 Boundary Conditions

One of the most important steps in a numerical simulation is the definition of appropriate boundary conditions. The use of wrong or unsuitable boundary conditions may drive us to misleading results. So, in the simulations, flow conditions were specified by imposing specific pressures at the inlet and outlet sections of the orifice. The fluid velocity at the walls was considered null and the walls itself were assumed adiabatic, what is consistent with the small dimensions and high speeds involved. This means that there is no time for a fluid particle to exchange heat with the walls. The different simulations were carried out by first, keeping the back pressure constant, at atmospheric pressure, and increasing the inlet pressure, and second, keeping the inlet pressure constant at atmospheric conditions and decreasing the back pressure to vacuum conditions.

3 VALIDATION OF THE NUMERICAL RESULTS

There are very few references in the literature related to simulation of flows in such small orifices and capillaries (small Reynolds numbers) with high-speed flow. Consequently, *a priori*, authors did not know if the solver could be an appropriate tool for this investigation. So, it was considered that an essential step in simulating the flows through the microorifices was the validation of the solver.

This validation was performed by comparing numerical to the experimental results obtained by Kawakita [1]. The only experimental results available were integral properties of the flow, in this case the volumetric flow rate refered to the upstream stagnation conditions (Q_0). Since the solver is capable of calculating the velocity, density, pressure and temperature field, the flow rate was computed by integrating the mass flux (flow velocity versus the gas density) across a section of the domain at different pressure ratios, for both operations under vacuum and under pressure. The results obtained can be seen in figures 2, 3 and 4.

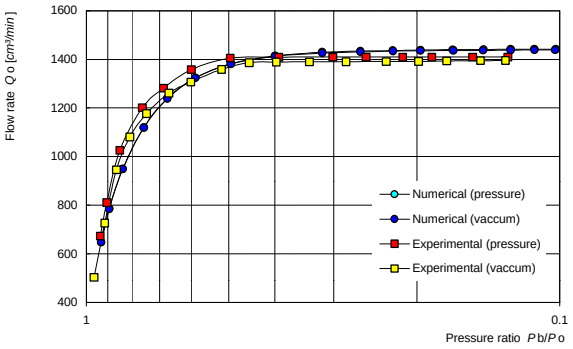

Figure 2. Experimental and numerical data of flow rates for a 423mm diameter orifice with L/D=0,6. Operation under pressure and under vacuum.

In the cases of figures 2 and 3, flow was assumed turbulent in the simulations. In contrast, simulation results presented in figure 4, were obtained assuming a laminar flow since the diameter of 16µm is quite small and, therefore, the Reynolds number is low.

Figure 2 basically represents the results of a small diameter orifice plate. The numerical and experimental results agree very well and the flow is clearly choked, i.e., there is no increase in volumetric flow rate with a decrease in the back to upstream pressure ratio.

The numerical results presented in figure 3 also agree reasonably well with the experimental values, presenting differences not larger than 10%. To explain this small difference between both methods, it should be pointed out that the inner surface roughness was not taken into consideration in the simulations. This means that, due to the small dimensions involved, the relative roughness is fairly large, and friction effects do indeed reduce the volumetric flow rate, providing lower values for the experimental results when compared to the results obtained by the simulation process.

In figure 4, experimental and numerical values of flow rates for a 16mm diameter orifice with L/D=16 are presented. Due to the very low flow rates involved and the test bench limitations, the experimental results for an operation under vacuum are not available and therefore, the numerical results could not be validated for this case. However, when operating under pressure, the results obtained numerically again agree reasonably well with those obtained experimentally.

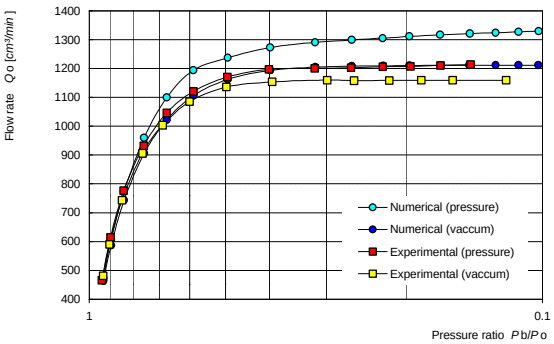

Figure 3. Experimental and numerical values of flow rates for a 427mm diameter orifice with L/D=16. Operations under pressure and under vacuum.

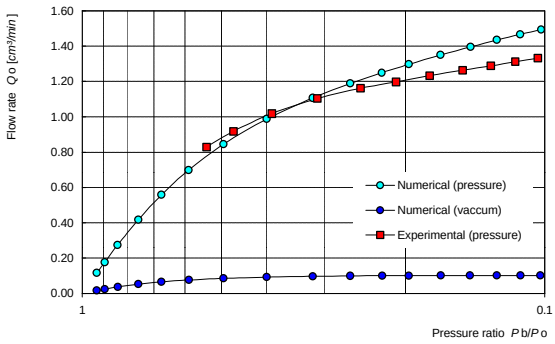

Figure 4. Experimental and numerical values of flow rates for a 16mm diameter orifice with L/D=16. Operations under pressure and under vacuum.

Figures 2, 3 and 4 show that there is a close agreement between numerical and experimental results. This fact indicates that probably the mathematical model used by the solver is appropriate for this kind of simulation and therefore, it can be used to study critical flow through small orifices, at least under the circumstances of this paper.

4 RESULTS

Given the appropriate boundary conditions and domain discretization, the result of a numerical simulation using finite-volumes formulation is a set of velocities, pressures, temperatures and other properties of the flow and the fluid itself at the different elements used in the discretization. Every other variable must be calculated from these properties.

4.1 Calculation of the volumetric flow rate

The mass flow rate through a surface may be calculated from a given velocity field by integrating the mass flux in the section as shown in equation (2) (Shapiro [2]):

$$\dot{m}_S = \int_S r\,\vec{v}\cdot\vec{n}dS \tag{2}$$

In equation (2), S represents the area, r the specific mass, $\vec{v}$ the velocity and $\vec{n}$ the outer normal to the surface. The volumetric flow rate under upstream stagnation conditions is calculated by dividing the mass flow rate by the specific mass at total conditions. Equation (2) was calculated in three different sections and an average value was adopted. It should be pointed out that the mass flow rate calculated in the different sections were always very close (typically within 1%) indicating that the solution was conservative. These results are plotted for the different orifices studied under different pressure conditions in figures 2, 3 and 4.

4.2 Velocity field

This section presents a few examples of velocity fields calculated. The colored velocity field allows a clear visualization of the flow. Figure 5 shows the velocity filed corresponding to the orifice studied in figure 2, with 423 mm and L/D=0,6. The results of operation under vacuum and under pressure with same back pressure to total pressure are very close (the only thing that changes is the specific mass, due to large differences in total pressure) and for this reason only the case of operation under pressure is presented.

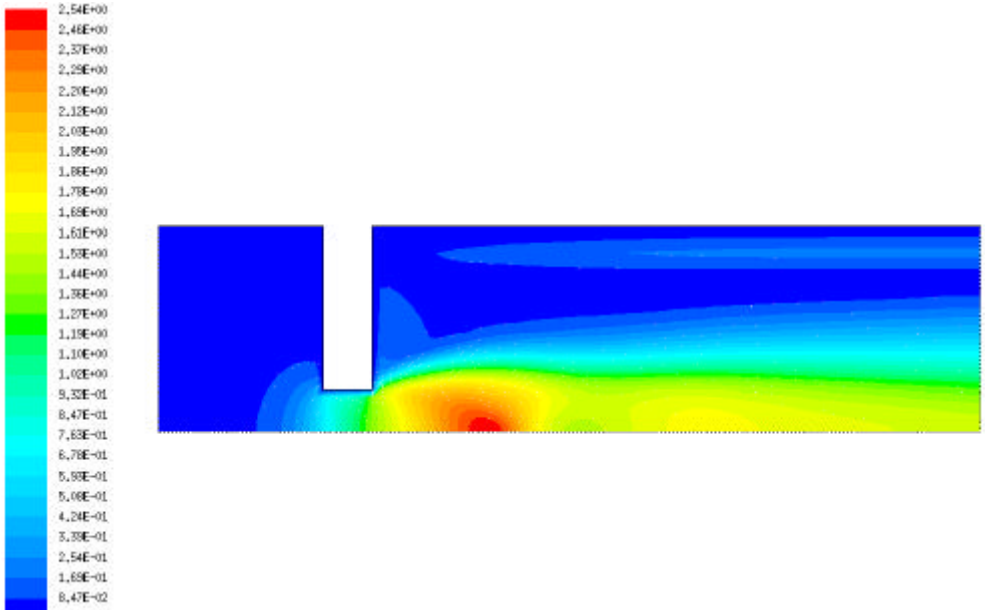

Figure 5. Velocity field (Mach number) for an orifice with 423mm and L/D=0,6. The usptream static pressure is 820 kPa and the back pressure is 0 kPa (atmospheric pressure).

Figure 6 shows the velocity field for an orifice with a diameter of 427*mm* and *L*/*D*=16. Again, the velocity field for operation under vacuum is very similar to operation under pressure and for this reason it is not presented.

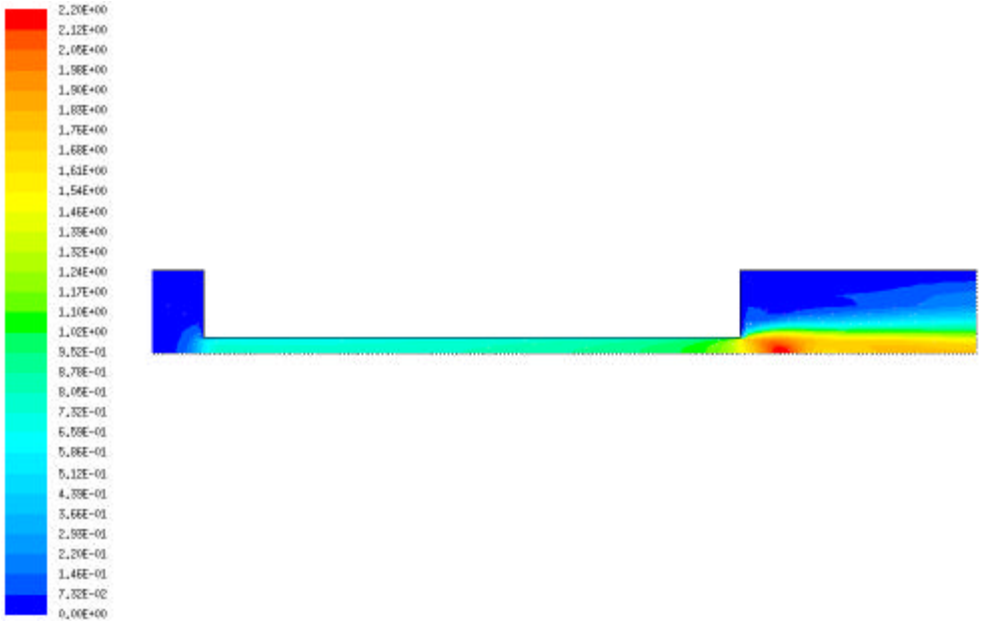

Figure 6. Velocity field (Mach number) for an orifice with 423*mm* and *L*/*D*=16. The upstream static pressure is 820 *kPa* and the back pressure is 0 *kPa* (atmospheric pressure).

Figures 7 and 8 show the velocity fields for an orifice with a diameter of 16*mm* and *L*/*D*=16. In this situation, a considerable difference in the velocity fields of operation vacuum and under pressure can be observed showing a difference in the flow pattern as a result of the Reynolds number.

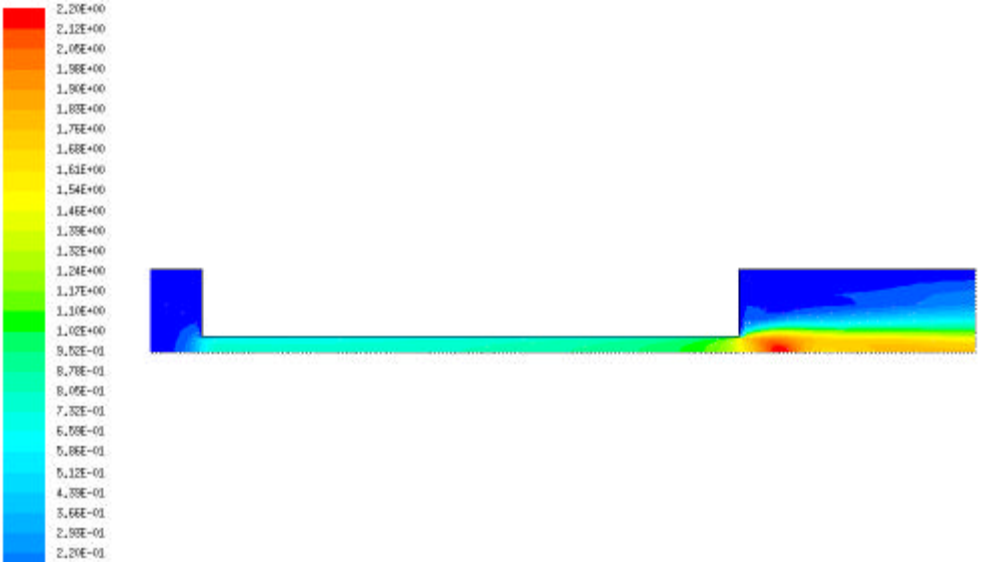

Figure 7. Velocity field (Mach number) for an orifice with 16*mm* and *L*/*D*=16. The upstream static pressure is 820 *kPa* and the back pressure is 0 *kPa* (atmospheric pressure).

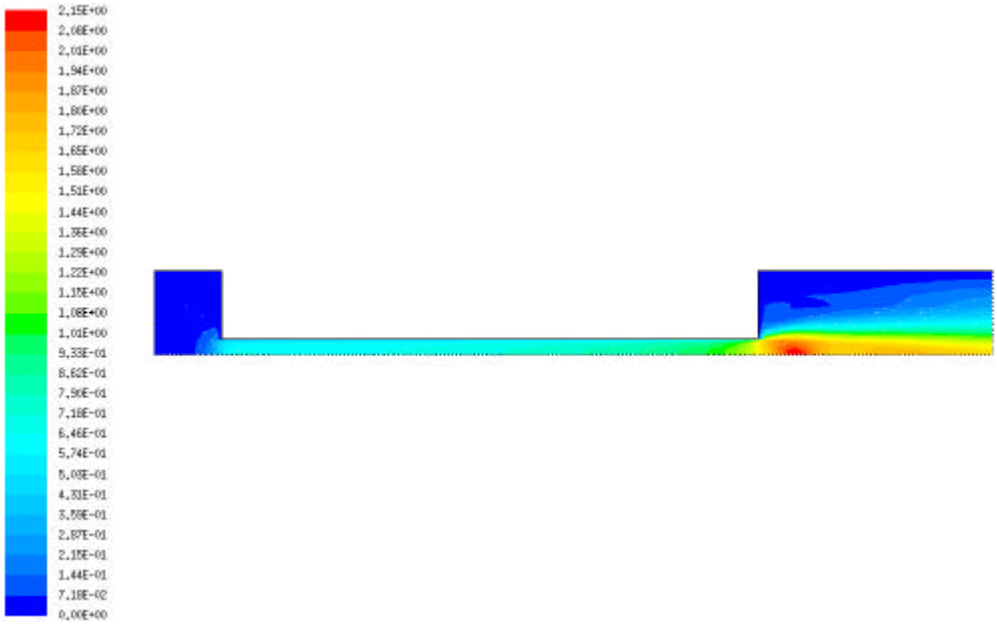

Figure 8. Velocity field (Mach number) for an orifice with 16*mm* and *L*/*D*=16. The upstream static pressure is 0 *kPa* (atmospheric pressure) and the back pressure is –83,5 *kPa*.

4.3 Velocity profiles

It is obvious from the previous figures that the flow behavior through small diameter orifices is different from that of large sized orifices. Transition from subcritical to critical regime is not easily observed and, as far as can be seen in figures 2, 3 and 4, the volumetric flow rate does not stabilize with decreasing values of back to total pressure ratios when operating under pressure. To investigate the effect of Reynolds number, velocity profiles were studied for the case of devices presenting ratios *L*/*D*=16, and the results obtained for the 16*mm* and 427*mm* diameters microorifices simulations were compared. The velocity profiles were fitted to the following equation:

$$\frac{V}{V_{max}} = 1 - \left(\frac{r}{R}\right)^n \tag{3}$$

Even though this equation is not very accurate, it does indicate quite well the “flatness” of the profile in a qualitative way as shown in figure 9, where different profiles with the exponent *n* varying from 2 to 10 are plotted. In equation (3), when *n* =2, the resulting velocity profile is the traditional laminar fully developed incompressible Poiseuille flow profile.

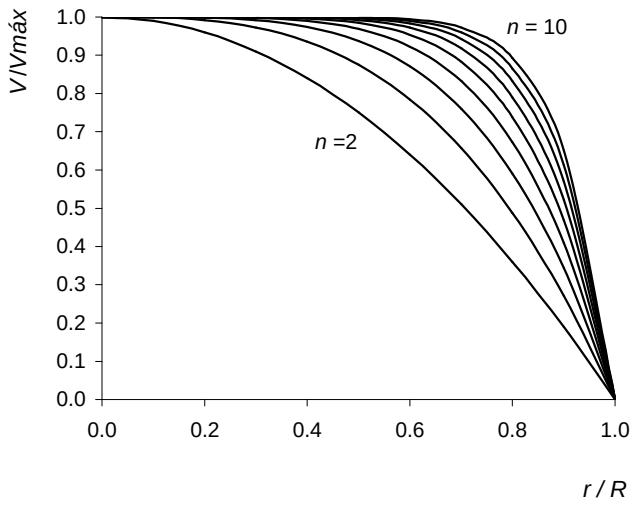

Figure 9. Non-dimensional velocity profiles according to equation (3) for *n* ranging from 2 to 10.

Figure 10 shows for the *L*/*D*=16 and *D*=16*mm* microorifice, the values of *n* for different positions along the axis. In figure 10, a laminar flow was assumed and in figure 11, a k-ε model was used. Notice that these profiles are only representative away from the borders (*L*/*D*=1 and *L*/*D*=16). This is due to the fact that near the borders the radial components of the velocity profile are not negligible.

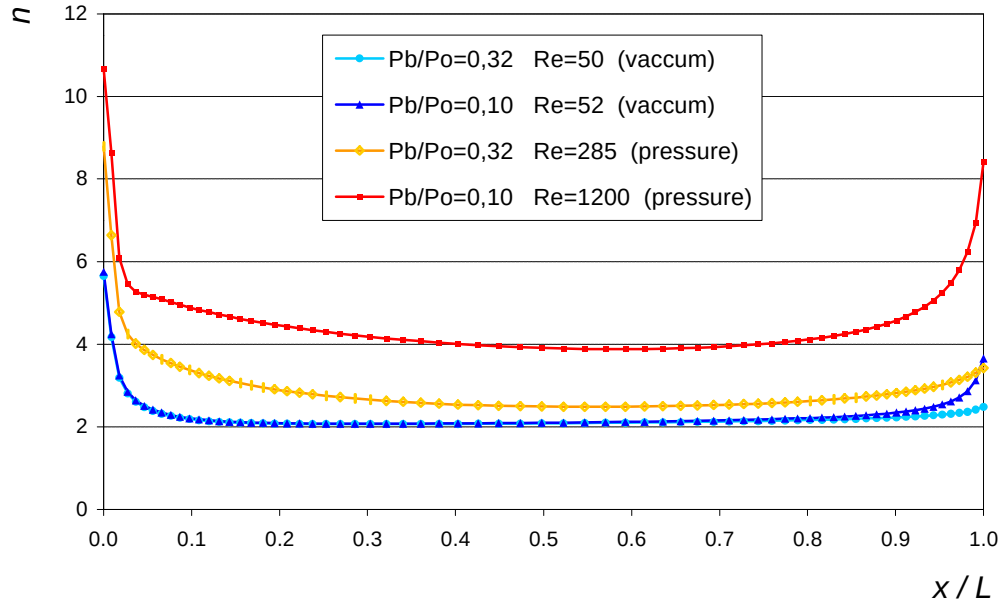

Figure 10. Velocity profile along the *L*/*D*=16 and *D*=16*mm* microorifice for different pressure and Reynolds number conditions.

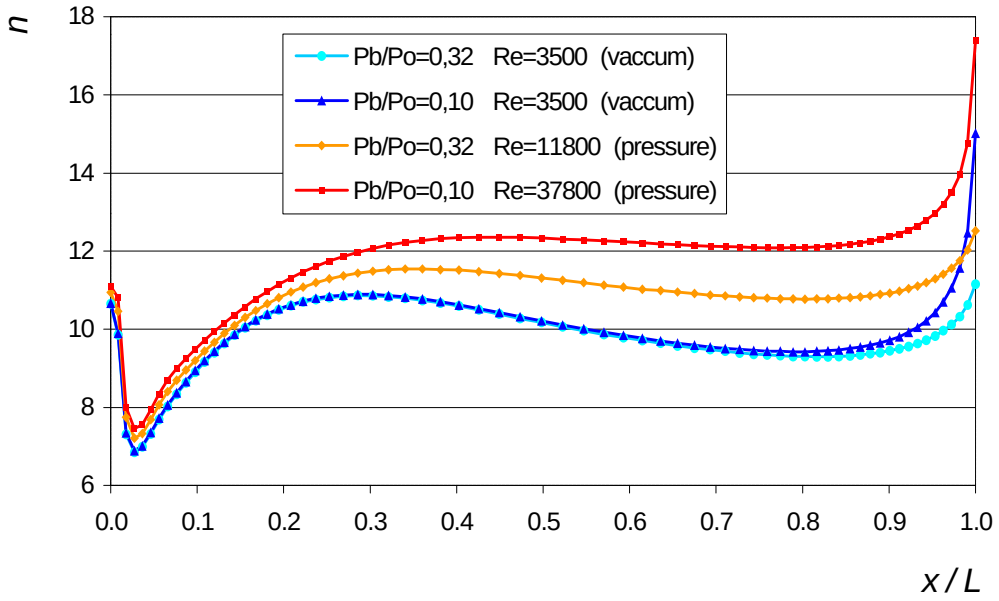

Figure 11. Velocity profile along the *L*/*D*=16 and *D*=427µm microorifice for different pressure and Reynolds number conditions.

Figures 10 and 11 show that when operating under vacuum, the Reynolds number does not vary and neither does the *n* factor. On the other hand, when operating under pressure, there is a noticeable difference in Reynolds number and the *n* exponent for different back to total pressure ratios.

It is important to remember that the model developed in this section is qualitative and only tries to explain the general behavior of the velocity profiles in the different situations analised in this paper.

5 DISCUSSION AND CONCLUSIONS

Results presented in section 4 show that, for small orifices there is a definite dependence of the flow rate on the Reynolds number in critical regime. With a stable *n* value for different back to total pressure ratios, the velocity profiles do not change and therefore, the volumetric flow rate related to the upstream stagnation conditions remains constant. This characteristic can be clearly seen in figures 2, 3 and 4. It is easy to see that when operating under vacuum the Reynolds number is almost constant. The mean velocity does not change that much, since the velocity is limited to sonic conditions, and the density of the gas does not change at all.

Conversely, when operating under pressure, there is a very large increase in density and Reynolds number. Figures 10 and 11 show that the velocity profile changes with Reynolds number and, as the Reynolds number increases, so does *n*. It should be remembered that close to the outlet of the orifice the flow velocity is limited by the speed of sound of the gas, which is confirmed by the velocity fields in figures 5, 6, 7 and 8, and therefore, an increase in *n* corresponds to an increase in the volumetric flow rate. As the diameter increases, the value of *n* also increases but, according to figure 9, for larger values of *n*, an increase in *n* leads to a comparatively smaller increase of the volumetric flow rates. This effect can be seen in figure 3 where, for an operation under pressure, the total volumetric flow rate continues to rise slightly as the back to total pressure ratio decreases. In figure 2, since the length to diameter ratio is very small, this effect is minimized and is barely noticeable.

This study shows that as the size of the restriction element decreases, critical condition can be established, but this condition changes considerably with Reynolds number. The extent that the flow rate depends on the Reynolds number is analogous to the behavior of the friction coefficient (and hence the flow rate if inlet and outlet pressures in a tube are kept constant) in tubes. For small Reynolds numbers, the friction coefficient depends strongly on the Reynolds number. In fact, for laminar incompressible flow, the friction coefficient *f* is given by $f=64/Re$. For large values of Reynolds number, the friction coefficient depends solely on the relative roughness.

These effects are related to the boundary layer thickness, which depends on the Reynolds number. When the Reynolds number is small, the boundary layer is thick and any change in Reynolds number will affect the velocity profile and, directly, the volumetric flow rate. When Reynolds number is large, the boundary layer is very thin and the velocity profile dependence on Reynolds number influences very little the volumetric flow rate. In fact, for high Reynolds number, potential isoentropic models predict very well the behavior of the flow pattern, as can be noticed in the large values of discharge coefficients present in sonic nozzles, where this parameter assumes values close to unity.

The measurement and control of very low gas flow rates are very difficult tasks to say the least. Undoubtedly, the use of microorifices allows real time flow measurements, but care should be taken concerning to some aspects. The effect of Reynolds number should be taken into consideration and it should be remembered that a major problem with microorifices and capillaries is the manufacturing process. Most processes produce the orifices and even nozzles one by one, and in this case dimensional control is very difficult, what makes important the calibration of each device produced. Probably, application of some recent technologies such as LIGA process could allow the manufacture of many identical orifices contributing to solve this problem.

Authors recognize that improvements should be done to this study. For instance, it is very important to consider a correct surface roughness, even though this parameter does not influence laminar flows in continuum problems when using the Navier-Stokes equations. Other types of geometries could also be investigated, such as convergent or convergent/divergent nozzles, and even in this case of “aerodynamic profiled devices”, the treatment to the problem should be different from the case of large nozzles since, due to the boundary layer effects, current isoentropic hypothesis are no longer valid.

Finally, this work shows that computational fluid dynamics tool is a fairly good and cheap option for investigation of flow in microdevices.

REFERENCES

[1] Kazuto, Kawakita, *Estudo Sobre Escoamentos Críticos e em Microorifícios e Capilares*, PhD. Thesis, Escola Politécnica da USP, 1999.

[2] Shapiro, A. H., *The Dynamics and Thermodynamics of Compressible Flow*, John Wiley & Sons, v1 and 2, New York, 1954.

[3] Anderson, J. D., *Modern Compressible Flow with Historical Perspectives*, McGraw Hill, New York, 1982.

[4] FLUENT Inc., *FLUENT 4.4 User Guide*, Fluent Inc., 1998.

[5] FLUENT Inc., *FLUENT 4.4 Reference Guide*, Fluent Inc., 1998.

[6] Anderson, J.D., *Computational Fluid Dynamics: The Basics with Applications*, 6th ed., McGraw Hill, New York, 1995.

ACKNOWLEDGEMENTS

Authors would like to thank Mr. Paul Baillio from BIRD PRECISION company and PADC/FINEP for the support to this investigation.

AUTHORS: Eng. Paulo José Saiz Jabardo and Dr. Kazuto Kawakita
IPT-Institute for Technological Research / Flow Laboratory
Cidade Universitária São Paulo / SP
05508-901 BRAZIL
Phone: 55-11-3767-4756
e-mail: pjabardo@ipt.br and kawakita@ipt.br